DESIGN ISSUES FOR THE OPTICAL TRANSITION RADIATION SCREENS FOR THE ELI-NP COMPTON GAMMA SOURCE

M. Marongiu*[1], A. Giribono[1], A. Mostacci[1], L. Palumbo[1], Sapienza University, Rome, Italy
V. Pettinacci, INFN, Rome, Italy
D. Alesini, E. Chiadroni, F. Cioeta, G. Di Pirro, V. Lollo, L. Pellegrino, V. Shpakov, A. Stella, C. Vaccarezza, A. Variola, LNF-INFN, Frascati, Italy
A. Cianchi, INFN-Roma "Tor Vergata"
[1]also at INFN, Rome, Italy

Abstract

A high brightness electron Linac is being built in the Compton Gamma Source at the ELI Nuclear Physics facility in Romania. To achieve the design luminosity, a train of 32, 16 ns spaced, bunches with a nominal charge of 250 pC will collide with the laser beam in the interaction point. Electron beam spot size is measured with optical transition radiation profile monitors. In order to measure the beam properties along the train, the screens must sustain the thermal stress due to the energy deposited by the bunches; moreover the optical radiation detecting system must have the necessary accuracy and resolution. This paper deals with the analytical studies as well as numerical simulations to investigate the thermal behavior of the screens impinged by the nominal bunch.

INTRODUCTION

The Gamma Beam Source [1] (GBS) machine is an advanced source of up to ≈20 MeV Gamma Rays based on Compton back-scattering, i.e. collision of an intense high power laser beam and a high brightness electron beam with maximum kinetic energy of about 740 MeV. The Linac will provide trains of bunches in each RF pulse, spaced by the same time interval needed to recirculate the laser pulse in a properly conceived and designed laser recirculator, in such a way that the same laser pulse will collide with all the electron bunches in the RF pulse, before being dumped. The final optimization foresees trains of 32 electron bunches separated by 16 ns, distributed along a 0.5 µs RF pulse, with a repetition rate of 100 Hz.

OPTICAL TRANSITION RADIATION (OTR) SCREEN

Optical Transition Radiation screens are widely used for beam profile measurements. The radiation is emitted when a charged particle beam crosses the boundary between two media with different optical properties, here a thin reflecting screen (e.g. a thin layer of aluminum sustained by a Si wafer) and vacuum. For beam diagnostic purposes the visible part of the radiation is used; an observation geometry in backward direction is chosen corresponding to the reflection of virtual photons at the screen which acts as mirror. The screen has an inclination angle of 45° with respect to the beam axis, and observation is performed at 90°. In a typical monitor setup the beam is imaged via OTR using standard lens optics, and the recorded intensity profile is a measure of the particle beam spot. Typical beam measurement in a high brightness linac involving OTR screen are measurement of bunch length [2], of Twiss parameters [3] or in general 6D characterization on bunch phase space [4].

Each ELI-GBS diagnostic station is equipped also with YAG screens.

THERMAL ANALYSIS

When a single particle hits a surface it deposits an amount of energy ΔE following the well known equation:

$$\Delta E = \frac{\partial E}{\partial z}\rho\Delta z \quad (1)$$

ρ is the density of the material and Δz is its thickness; the stopping power $\partial E/\partial z$ depends on the material and on the particle energy while it can be considered spatially independent: we assume for it a value of 2 MeV*cm^2*g^{-1} [5]; other references use instead a value of 1.61 MeV*cm^2*g^{-1} [6] or 1.64 MeV*cm^2*g^{-1} [7]. There are also numerical code able to evaluate the stopping power, e.g. the EGS4 code [8].

Assuming an electron beam with a Gaussian spatial distribution, the time evolution of the target temperature can be calculated solving the equation [9]

$$\frac{\partial T(r,t)}{\partial t} = \frac{1}{c_p\rho}\left\{\frac{\partial E}{\partial z}\rho\exp\left(-\frac{r^2}{2\sigma_x\sigma_y}\right)eN(t) - k\nabla^2 T(r,t) - \frac{2\epsilon\sigma_{sb}}{\Delta z}\left[T(r,t)^4 - T_0^4\right]\right\} \quad (2)$$

where the first addendum represents the temperature rising, while the second one is the cooling by conduction and the third one is the radiation cooling. r is the position of the beam, σ_x (σ_y) represents the beam size; c_p is the specific heat, $N(t)$ is the charge distribution of the beam, k is the thermal conductivity, ϵ is the emissivity and σ_{sb} is the Stephan-Boltzmann constant.

Temperature Increase

When a bunch hits the OTR, with the hypothesis of a beam with a Gaussian spatial distribution, it rises its tem-

* marco.marongiu@uniroma1.it

perature according to [5]

$$\Delta T^{+}(r) = \frac{\partial E}{\partial z}\frac{eN}{c_p \pi \sigma_x \sigma_y}\exp\left(-\frac{r^2}{2\sigma_x\sigma_y}\right) \quad (3)$$

The temperature rising depends linearly on the bunch charge and inversely on the specific heat. Furthermore it varies with the dimension of the beam: a more focused beam causes more heating as we can see from the Figures 1 and 2 which refer to a single bunch impulse. All the numerical calculations and the plots in this paper have been made using the values taken from "Matweb" [10] for the specific heat and the other parameters of the materials.

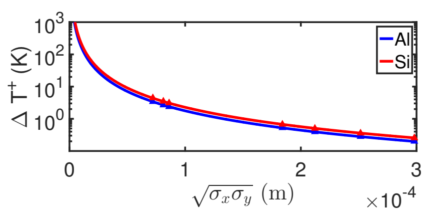

Figure 1: Instantaneous temperature rising as a function of the beam dimension for two different material (Aluminum and Silicon) and a bunch charge of 250 pC. The triangles represent the values at the position of OTR stations in the ELI-GBS (see Table 1).

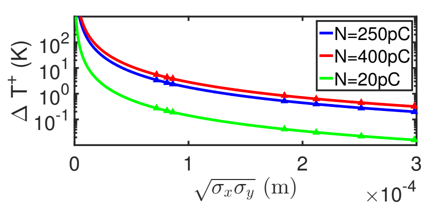

Figure 2: Instantaneous temperature rising in an aluminum target as a function of the beam dimension for three different values of the bunch charge (20 pC, 250 pC and 400 pC). The triangles represent the values at the position of OTR stations in the ELI-GBS (see Table 1).

Cooling Mechanism

There are two cooling mechanism for the OTR screens, conduction and radiation: since we are in a vacuum chamber there is not convection term. The radiation cooling, however, can be considered negligible for temperature below 1000 K; therefore we will take into account only the conduction cooling effects. Moreover we can neglect the cooling effect between bunches, since we have a bunch separation of only 16 ns, and we consider only the cooling between macro-pulse which has a separation of 10 ms. The two dimensional heat conduction equation is [6]

$$\frac{\partial T}{\partial t} = \alpha_d \nabla^2 T + \frac{1}{\rho c_p} q(x,y,t), \qquad \alpha_d = \frac{k}{\rho c_p} \quad (4)$$

α_d being the thermal diffusivity. We are assuming the following condition:

- The cooling mechanism considered is only the heat transfer from the heated area to the other part of the screen (in ELI-GBS linac the rms beam size $\sigma_{x,y} \in [10, 300]$µm and the OTR screens have the dimension of 30 mm x 30 mm). Thus we consider the temperature of the flange as independent on the temperature of the heated area and equal to the room temperature [6].
- The density of the internal heat source $q(x,y,t)$ has a Gaussian form (as a function of x and y) during the passage of the electron bunch through the material slab [6].

The solution of Equation 4 is

$$\Delta T_{max}(t) = \frac{\sigma_x}{\sqrt{2\alpha_d t + \sigma_x^2}}\frac{\sigma_y}{\sqrt{2\alpha_d t + \sigma_y^2}}\Delta T_{max}(0) \quad (5)$$

which allows us also to estimate the time needed to cool

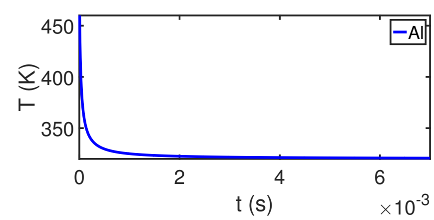

Figure 3: Temporal evolution of the conduction cooling after the heating of a train impulse like the one at ELI-GBS (σ_x =47.5 µm, σ_y =109 µm).

down. Since the frequency rate in ELI-GBS linac is 100 Hz, the OTR can't completely cool down in the time between two subsequent pulses. However, as shown in Figure 3, we can see that after 10 ms from the bunch train, the temperature is 320.3 K for the aluminum and 320.4 K for the silicon, which are close enough to the rest values. In the Table 1 we show the instantaneous temperature rise caused by beam of different spot size with 32 bunches with a charge of 250 pC each, emphasizing the worst case.

Table 1: Instantaneous Temperature Increase for a Impulse Train of 32 Bunches with a Charge of 250 pC Each. We Also Emphasized the Worst Case Scenario for the ELI-GBS.

$\sigma_x(\sigma_y)$[µm]	ΔT^+ Al [K]	ΔT^+ Si [K]
298 (298)	6	8
251 (252)	9	12
211 (213)	12	16
184 (184)	17	21
47.5 (109)	**113**	**141**
241 (27.4)	85	110
106 (70)	76	99

ISBN 978-3-95450-147-2

ANSYS NUMERICAL ANALYSIS

To study the OTR behavior both in the steady state and in the transient regime, we perform a numerical simulation (ANSYS). We assume an input load in a little volume of the OTR, that is equivalent to the beam spot size, times the depth of the target (380 µm). For the steady state simulation, the input load is the internal heat generation, while for the transient study, we directly impose a temperature increase. The simulation are performed on a bulk Al screen, since the effect does not depend on the thickness of the screen, as shown in Equation 5.

The first simulation concerns the study in the steady state of the OTR behavior for 10 ms considering an internal heat generation of 84×10^9 Wm^{-3} as input: this value is equivalent to the average power that will be deposited by the ELI-GBS beam in a 10 ms time interval according to Equation 1. In this case we have achieved the results expected: at the thermal equilibrium we have only one degree more over the initial temperature (see Figure 4). This result, at this stage of our analysis, is acceptable in order to compare the theoretical study and the ANSYS simulation study.

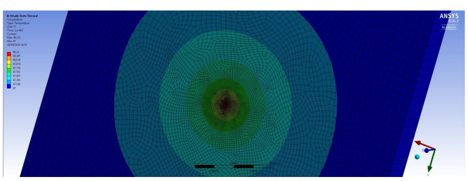

Figure 4: ANSYS results at the equilibrium condition considering an internal heat generation of 84×10^9 Wm^{-3} in a little cylinder 380 µm thick and 47.5 µm,109 µm large. This dimension are the one expected during operation at the ELI-GBS (Al bulk screen).

We also perform the thermal transient analysis using a load temperature of 160 K: however, in this case, the result of the simulation is slightly different from the expected one (see Figure 5). Indeed, the ANSYS simulation shows a cooling faster than the expected theoretical one; more studies are needed to better understand such differences.

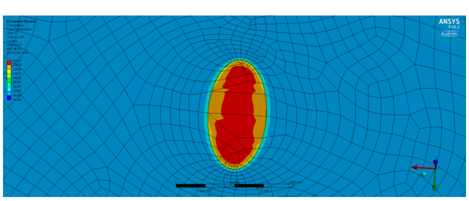

Figure 5: ANSYS results of the thermal transient analysis using a load temperature of 160 K in a little cylinder 380 µm thick and 47.5 µm,109 µm large. This dimension are the one expected during operation at the ELI-GBS (Al bulk screen).

THERMAL STRESS

Due to beam energy deposition on the OTR targets we expect an instantaneous temperature increase of 113 K for the aluminum and of 140 K for the silicon in the worst case scenario. The thermal stress limit is given by

$$\Delta T_{stress} \approx \frac{2\sigma_{ten}}{\alpha E_y} \tag{6}$$

where σ_{ten} is the ultimate tensile strength, α is the coefficient of thermal linear expansion and E_y is the Young's Modulus. From Equation 6 it follows that the maximum instantaneous temperature increase is 130 K for the aluminum and 1200 K for the silicon.

The cycling of the screen temperature between this two different values may induce failure according to Basquin equation [11]. For ELI-GBS, in the worst case scenario, we may have a mean time before failure (MTBF) of about 20 ms. For SPARC parameters [12], instead, we find a value above 2×10^{14} years. We can also choose targets made of silicon alone like the ones at DESY [6]: in this case, we find out that the MTBF is around 2 years for the "ELI-GBS case", and it goes up to about 3×10^{21} years at SPARC. In Table 2 we summarized this results.

Table 2: This Value Refers to a Starting Temperature T_0 of 320 K.

LINAC	ΔT^+	**MTBF**
SPARC	0.5 K	2×10^{14} years
ELI-GBS (Al)	113 K	20 ms
ELI-GBS (Si)	146 K	2 years

CONCLUSION

Spot size measurements for nominal ELI-GBS beam may damage the aluminum layer of the OTR screen: the temperature rise caused by the 32 bunches-pulse has been estimated of 113 K, which is below the melting point but very close to the maximum temperature allowed by bulk aluminum that is 119 K. The expected lifetime for Al-Si OTR screens is too short for nominal ELI-GBS operation. YAG screens will be used for single bunch measurement, while bulk silicon for full train characterization.

REFERENCES

[1] A. Bacci, D. Alesini, P. Antici *et al.*, "Electron linac design to drive bright Compton back-scattering gamma-ray sources," *Journal of Applied Physics*, vol. 113, no. 19, p. 194508, 2013.

[2] D. Filippetto, M. Bellaveglia, M. Castellano *et al.*, "Phase space analysis of velocity bunched beams," *Physical Review Special Topics-Accelerators and Beams*, vol. 14, no. 9, p. 092804, 2011.

[3] A. Mostacci, M. Bellaveglia, E. Chiadroni *et al.*, "Chromatic effects in quadrupole scan emittance measurements," *Physical Review Special Topics-Accelerators and Beams*, vol. 15, no. 8, p. 082802, 2012.

[4] A. Cianchi, D. Alesini, M. Anania *et al.*, "Six-dimensional measurements of trains of high brightness electron bunches,"

Physical Review Special Topics-Accelerators and Beams, vol. 18, no. 8, p. 082804, 2015.

[5] E. Bravin, “Thermal Analysis of OTR Screens for CTF3,” CERN, Geneva, Switzerland, Tech. Rep. CTF3-Note-019, March 2001.

[6] V. Balandin and N. Golubeva, “Survival and thermal heating of materials for the OTR screens at the TTF2,” 2001, unpublished.

[7] A. Variola, “Utilisation du rayonnement optique pour l’etude des caracteristiques spatiotemporelles d’un faisceau d’electrons. Application a TTF,” Ph.D. dissertation, Universite de Paris-Sud, France, 1998.

[8] W. Nelson and Y. Namito, *The EGS4 Code System: Solution of Gamma-Ray and Electron Transport Problems*. SLAC, 1990.

[9] E. Bravin, T. Lefevre, and C. Vermare, “OTR Studies for the High Charge CTF3 Beam,” in *Particle Accelerator Conference, 2003. PAC 2003. Proceedings of the*, vol. 4. IEEE, 2003, pp. 2464–2466.

[10] Matweb materials information. [Online]. Available: http://www.matweb.com/

[11] R. I. Stephens, A. Fatemi, R. R. Stephens *et al.*, *Metal fatigue in engineering*. John Wiley & Sons, 2000.

[12] A. Bacci, F. Broggi, C. DeMartinis *et al.*, “Status of Thomson source at SPARC/PLASMONX,” *Nuclear Instruments and Methods in Physics Research Section A: Accelerators, Spectrometers, Detectors and Associated Equipment*, vol. 608, no. 1, pp. S90–S93, 2009.

ISBN 978-3-95450-147-2